

ACTINOID PNICTIDES—I

HEAT CAPACITIES FROM 5 TO 950 K AND MAGNETIC TRANSITIONS OF U_3As_4 AND U_3Sb_4 . FERROMAGNETIC TRANSITIONS†

A. ALLES,‡ B. G. FALK§ and EDGAR F. WESTRUM, Jr.

Department of Chemistry, University of Michigan, Ann Arbor, MI 48109, U.S.A.

and

FREDRIK GRØNVOLD and MORAD RAMZY ZAKI¶

Chemical Institute, University of Oslo, Blindern, Oslo 3, Norway

(Received 22 February 1977)

Abstract—The heat capacities of triuranium tetraarsenide (U_3As_4) and triuranium tetraantimonide (U_3Sb_4), measured by adiabatic calorimetry over the temperature range 5–950 K, show sharp λ -shaped transitions at 196.1 and 147.5 K, respectively. The maxima are related to the appearance of permanent magnetic moments below 198 and 148 K. Excess cooperative entropies associated with ferromagnetic ordering are tentatively estimated as 6.7 for U_3As_4 and 6.8 cal K^{-1} mole $^{-1}$ for U_3Sb_4 . These are larger than the two literature values reported for U_3P_4 (1.5 and 3.1 cal K^{-1} mole $^{-1}$). The fact that these entropy of transition values are much smaller than would be expected from $\Delta S_i = R \ln(2J + 1)$ for the 3H_4 ground term ($J = 4$) and that the observed heat capacities at high temperatures are much larger than would be expected from lattice plus dilational contributions are evidence of crystal field effects. The total electronic entropies to 950 K are estimated as 11.05 and 12.95 cal K^{-1} mole $^{-1}$ for U_3As_4 and U_3Sb_4 , respectively. Thermal functions for both U_3As_4 and U_3Sb_4 are integrated from the experimental data up to 950 K. At 298.15 K, the values of C_p , $[S^\circ(T) - S^\circ(0)]$ and $-[G^\circ(T) - H^\circ(0)]/T$ in cal K^{-1} mole $^{-1}$, are 44.82, 73.87 and 38.97, U_3As_4 and 44.98, 83.60 and 46.89, for U_3Sb_4 .

INTRODUCTION

There has been increased interest in the magnetic and thermophysical properties of uranium pnictides (U_3X_4) in which X = P, As, Sb, or Bi; all of which have cubic Th_3P_4 -type structures[1]. Magnetic susceptibility and magnetization measurements[2–12] show that they all order to a ferromagnetic state below 300 K and that the Curie–Weiss law is obeyed above the Curie temperature (T_C) up to at least 400 K. The paramagnetic moment increases with increasing pnigogen size, but lack of such a correlation for the ordering temperature might indicate that the magnetic coupling is anomalously weak in U_3P_4 .

The U^{4+} site in U_3X_4 has S_4 symmetry which splits the nine-fold degenerate 3H_4 ground term into five singlets and two doublets. Troc *et al.*[3] calculated the energy levels of the ground term using a point charge model and obtained a good correlation with their high-temperature magnetic susceptibility data. The lowest excited level, a singlet at 9 cm^{-1} above the singlet ground level is followed by seven higher levels, the lowest of which is at 700 cm^{-1} .

Single crystals of U_3As_4 [13] are semi-metallic with a resistivity of 490 $\mu\Omega$ cm at 300 K while U_3Sb_4 is reported

to be metallic[1]. Low-temperature heat-capacity data for U_3P_4 [14, 15] have been reported in two works, which disagree by a factor of two on the entropy of transition (ΔS_i).

In the present paper we report heat-capacity data for U_3As_4 and U_3Sb_4 over the temperature range 5–950 K and deduce enthalpies and entropies for the magnetic disordering process and for the total electronic contribution.

EXPERIMENTAL

Samples. The compounds were obtained in a two-step synthesis involving direct combination of appropriate amounts of high purity uranium metal and pnigogens described earlier[16, 17]. First, the dipnictides, UX_2 , were prepared by heating a uranium–pnigogen mixture of molar ratio 1:2 within evacuated, sealed, silica tubes in a muffle furnace[17]. Second, the diarsenide batches were heated under vacuum (10^{-6} torr) to (1100 \pm 10) K for 4d, while the antimonide was heated to (1290 \pm 10) K for 12 d. Only that portion of the long tube containing the dipnictide was heated by a tube furnace. The resulting U_3X_4 was then transferred to the high-temperature calorimeter tube for tempering at 820 K for 7d. After completion of the high-temperature heat-capacity measurements, the samples were transferred under an anhydrous nitrogen atmosphere to a gold-plated copper calorimeter for low-temperature measurements. X-Ray powder photographs of the samples were taken with Guinier-type focusing cameras of 80 mm diameter and CuK_{α_1} -radiation. Potassium chloride (AnalaR) was used as a calibration substance (a (20°C) = 629.19 μm [18]). The lattice constants are $a = (852.0 \pm 0.3)$ μm for U_3As_4 and $a = (911.1 \pm 0.3)$ μm for U_3Sb_4 . They accord well with those reported earlier for U_3As_4 by Iandelli[19] (852.4 μm), Trzebiatowski *et al.*[2] (853.1 μm) and Warren and Price[20] (852.80 \pm 0.05) μm for a sample prepared at 1200°C, and for U_3Sb_4 by Ferro[21] ($a = 909.5$ μm).

†This research was supported in part by the Chemical Thermodynamics Program, Chemistry Section, National Science Foundation under Contract No. GP-42525X.

‡Present address: Department of Chemistry, UFSC, 88000 Florianopolis, Brazil.

§Present address: Thermochemistry Laboratory, Chemical Center, University of Lund, S-220 07 Lund, Sweden.

¶Present address: Nuclear Chemical Department, Atomic Energy Establishment, Inshas, Egypt.

Heat capacities 3–350 K, University of Michigan. The heat capacities of U_3As_4 and U_3Sb_4 have been measured in the adiabatic calorimeter described previously[22]. For the measurements, about 157 g of U_3As_4 and 153 g of U_3Sb_4 were used. The heat capacity of the samples represented from 60 to 70% of the total. The energetics of the transitions were reproducible within 0.1%. After each energy input in the transition region thermal equilibrium was obtained within 10 min. The rate of heating and cooling did not affect the results; no change in results was seen after the samples were taken to 4 K.

Heat capacities 300–950 K, University of Oslo. The calorimetric apparatus and measuring technique have been described[23]. The calorimeter was intermittently heated, and surrounded by electrically heated and electronically controlled adiabatic shields. The substance was enclosed in an evacuated and sealed silica glass tube of about 50 cm³ volume, tightly fitted, into the silver calorimeter. A central well in the tube served for the heater and platinum resistance thermometer. The same amount of samples as for the low-temperature calorimeter was used and the heat capacity of the samples represented only 25–30% of the total heat capacity.

Calibrations and adjustments. The platinum resistance thermometer for the low-temperature calorimeter had been calibrated by the U.S. National Bureau of Standards, and that for the high-temperature calorimeter locally, at the ice, steam and zinc points. Temperatures are judged to correspond to IPTS-68 within 0.02 K from 4–300 K, and within 0.05 K above the temperature. Energy inputs were measured with reference to instruments calibrated by the U.S. National Bureau of Standards.

Small corrections were applied for temperature excursions of the shields from the calorimeter temperature and for “zero drift” of the calorimeter temperature. Further small corrections were applied for differences in amounts of indium–tin solder, helium gas and Apiezon-T grease for the low-temperature calorimeter and for differences in mass of the quartz containers for the high-temperature calorimeter.

RESULTS

The experimental heat capacities for the low- and high-temperature range are given in chronological sequence in Tables 1 and 2 and depicted graphically in Figs. 1 and 2. The enthalpy determinations are summarized in Table 3.

The heat-capacity determinations are expressed in terms of the calorie defined as 4.184 J, an ice point of 273.15 K, and the atomic mass of natural uranium 238.029 g mole⁻¹. The molar masses are taken as 1013.77 g mole⁻¹ for U_3As_4 and 1201.09 g mole⁻¹ for U_3Sb_4 . The heat-capacity values are considered to have a probable error of about 5% at 5 K, 1% at 10 K and less than 0.1% from 25 to 350 K, and 0.5% at higher temperatures. The results have been adjusted for curvature. Values of ΔT used for the determinations can usually be inferred from the increments between adjacent mean temperatures. Both substances showed λ -type transitions

Table 1. Low-temperature heat capacities of U_3As_4 and U_3Sb_4 ; (cal = 4.184 J)

T K	C_p cal K ⁻¹ mole ⁻¹	T K	C_p cal K ⁻¹ mole ⁻¹	T K	C_p cal K ⁻¹ mole ⁻¹	T K	C_p cal K ⁻¹ mole ⁻¹
U_3As_4 (molar mass/g = 1013.77)							
Series I		199.57	46.97	Series IV		29.31	6.784
		201.48	46.15			32.44	8.110
157.76	45.57	204.16	45.50	173.99	48.75	35.90	9.768
166.87	47.27	206.79	45.13	ΔH_i , Det'n B		40.14	11.80
175.69	49.16	213.72	44.59	220.70	44.33	43.93	13.67
184.24	51.24	224.89	44.30			48.46	15.87
192.47	54.28	235.99	44.25	Series V		53.70	18.29
198.28	48.52	247.07	44.35	192.77	54.27	59.73	20.98
201.84	46.03	258.11	44.49	193.57	54.73	66.60	23.80
205.42	45.26	269.10	44.65	194.03	54.89	72.63	25.96
211.74	44.68	280.03	44.68	194.48	55.35		
220.80	44.36	290.97	44.77	194.82	55.58	Series VII	
		301.87	44.80	195.04	55.86	114.72	37.30
Series II		312.70	44.95	195.27	56.29	ΔH_i , Det'n C	
		323.49	45.08	195.49	56.20	167.64	47.48
121.31	38.69	334.27	45.16	195.71	56.76	176.66	49.36
131.15	40.64	344.65	45.20	196.04	57.21	ΔH_i , Det'n D	
140.57	42.42			196.50	52.33	218.78	44.46
149.66	44.12	Series III		196.97	49.21		
158.45	45.75			197.46	48.35	Series VIII	
166.97	47.40					179.39	49.99
175.26	49.08			Series VI		182.32	50.68
180.94	50.35	65.38	23.33	4.53	0.08	185.20	51.47
183.07	51.02	71.86	25.73	4.96	0.08	188.59	52.50
184.11	51.22	79.57	28.38	6.22	0.13	192.38	54.13
185.15	51.49	86.53	30.60	7.83	0.21	194.80	55.67
186.19	51.72	93.76	32.54	8.85	0.30	195.50	56.69
187.22	51.98	100.58	34.21	10.02	0.42	195.74	56.96
188.25	52.30	108.24	35.93	11.36	0.538	195.97	57.32
189.28	52.66	116.69	37.75	12.54	0.697	196.20	56.44
190.30	53.06	124.76	39.38	13.72	0.908	196.45	52.84
191.31	53.44	132.53	40.88	14.91	1.168	196.72	50.13
192.31	54.08	141.20	42.52	16.15	1.448	196.98	49.45
193.31	54.62	150.76	44.24	17.55	1.867	197.23	48.99
194.30	55.32	159.99	45.94	19.52	2.512	197.49	48.33
195.27	57.14	166.32	47.09	21.63	3.295	197.76	47.91
196.25	54.26	173.69	48.75	23.86	4.205	198.02	47.43
197.34	48.84	ΔH_i , Det'n A		26.38	5.321		
198.46	47.67	220.41	44.37				

Table 1. (Contd)

T	C_p	T	C_p	T	C_p	T	C_p
K cal K ⁻¹ mole ⁻¹		K cal K ⁻¹ mole ⁻¹		K cal K ⁻¹ mole ⁻¹		K cal K ⁻¹ mole ⁻¹	
U ₃ Sb ₄ (molar mass/g = 1201.09)							
Series I		Series III		Series V		Series VII	
94.55	39.03	127.36	47.15	151.66	45.53	85.35	36.52
106.86	42.02	ΔH_f Det'n B		152.42	45.47	92.56	38.48
118.15	44.79	174.76	43.56	154.10	44.87	99.39	40.13
128.72	47.54	Series IV		Series V		Series VII	
138.73	50.80	Series IV		Series V		Series VII	
145.43	54.40	89.66	37.78			126.72	46.98
149.27	48.27	98.50	39.97	4.91	0.1	ΔH_f Det'n D	
153.34	45.04	106.83	42.02	5.49	0.09	179.30	43.57
157.55	44.31	ΔH_f Det'n C		6.40	0.14	Series VIII	
164.92	43.83	137.01	50.05	7.51	0.20	Series VIII	
175.36	43.61	138.35	50.47	8.73	0.34	Series VIII	
185.75	43.60	140.23	51.26	9.64	0.484	131.23	48.28
196.08	43.69	142.64	52.42	10.66	0.679	134.79	49.35
206.34	43.79	144.31	53.40	11.71	0.897	136.94	50.09
216.55	43.97	145.24	54.07	13.17	1.311	139.03	50.82
226.70	44.05	145.94	54.66	14.80	1.886	141.40	51.85
236.80	44.17	146.39	55.22	16.44	2.556	143.42	52.83
246.85	44.30	146.70	55.52	18.23	3.398	144.73	53.69
256.85	44.40	146.92	55.90	20.21	4.416	145.57	54.43
266.81	44.55	147.14	56.72	22.66	5.775	146.15	55.02
276.74	44.67	147.39	57.59	26.48	8.055	146.55	55.56
286.62	44.80	147.65	55.50	30.88	10.90	146.80	55.74
296.45	44.96	147.87	51.44			147.03	56.18
306.27	45.07	148.10	49.51			147.27	57.22
306.04	45.20	148.33	48.86	Series VI		147.52	57.23
325.80	45.21	148.57	47.96	Series VI		147.77	52.57
335.53	45.24	148.81	47.61	34.97	13.49	148.01	49.76
345.26	45.37	149.05	47.34	38.96	16.04	148.26	48.99
		149.32	46.91	42.34	18.12	148.49	47.83
		149.57	46.48	45.97	20.27	148.73	47.63
		149.83	46.39	49.85	22.45	148.97	47.31
		150.08	46.25	54.06	24.62	149.21	46.85
		150.32	46.03	58.70	26.84	149.73	46.53
		150.57	45.99	62.86	28.71	150.52	46.13
		150.81	46.10	66.77	30.27	151.30	45.72
		151.05	45.78	71.14	31.84	153.53	45.03
		151.30	45.70	77.63	34.05	157.62	44.36

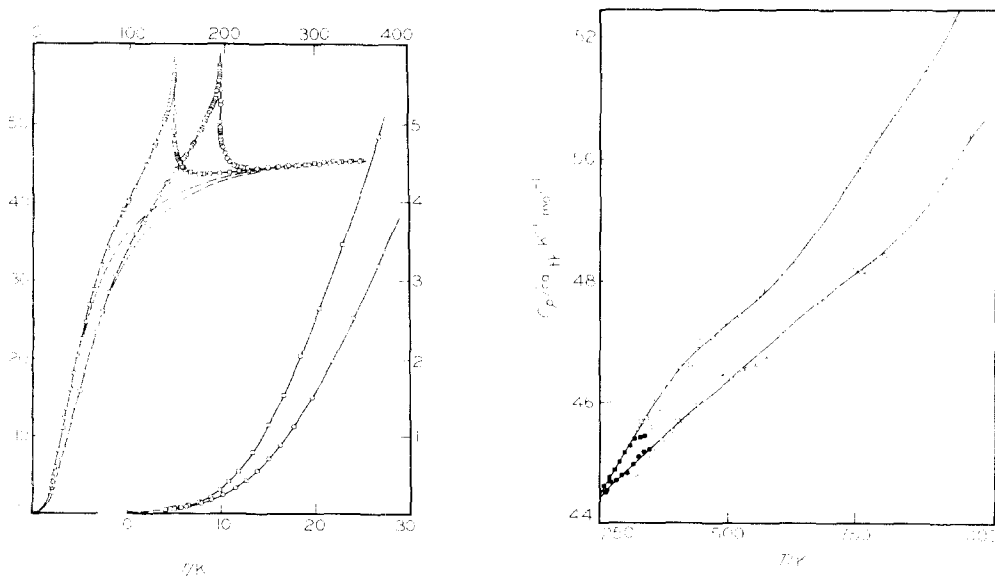


Fig. 1. High-temperature heat capacities for U₃As₄ ○, for U₃Sb₄ □, and lattice estimates —.

Fig. 2. High-temperature heat capacities for U₃As₄ ○, and U₃Sb₄ □. Overlapping low-temperature data are indicated by ●, and ■, respectively.

Table 2. High-temperature heat capacities of U_3As_4 and U_3Sb_4 ; (cal = 4.184 J)

T	C_p	T	C_p	T	C_p	T	C_p
K	cal K ⁻¹ mole ⁻¹	K	cal K ⁻¹ mole ⁻¹	K	cal K ⁻¹ mole ⁻¹	K	cal K ⁻¹ mole ⁻¹
U_3As_4 (molar mole/g = 1013.77)							
Series I							
		485.47	46.48	681.47	47.65	839.46	48.87
		496.16	46.43	692.64	47.72	851.30	48.65
316.24	44.72	506.89	46.38	703.86	48.03	863.21	48.94
326.87	44.77	517.64	46.61	715.12	47.92	875.13	49.20
337.47	44.90	528.41	46.54	726.44	48.20	885.90	49.49
348.07	45.05	539.17	46.56	737.79	48.28	897.82	49.49
358.65	45.21	549.88	46.63	749.11	48.20	909.74	49.76
369.22	45.36	560.59	46.63	760.52	48.15	921.68	49.66
379.77	45.32	571.38	46.76	772.07	48.13	933.70	49.76
390.31	45.51	582.22	46.74	783.68	48.30	945.85	49.56
400.85	45.69	593.12	46.86	795.33	48.40	958.04	50.06
411.39	45.66	604.07	47.11	807.03	48.43	970.23	50.39
421.94	45.74	615.06	47.21			982.46	50.46
432.48	45.98	626.08	47.13	Series II		1000.0	50.55
443.03	45.91	637.12	47.48			1010.0	50.72
453.60	46.03	648.18	47.61	804.22	48.28		
464.20	46.24	659.25	47.78	815.92	48.42		
474.82	46.34	670.34	47.62	827.68	48.40		
U_3Sb_4 (molar mass/g = 1201.09)							
Series I							
		469.40	46.88	644.03	48.43	831.09	50.56
		480.11	47.01	655.46	48.35	843.12	50.74
318.48	45.36	490.80	47.13	666.94	48.72	855.14	50.64
329.39	45.47	501.51	47.00	678.45	48.89	867.16	50.99
340.27	45.54	512.22	47.36	690.00	48.67	879.25	51.35
351.14	45.86	523.04	47.25	701.59	49.14	891.38	51.23
361.98	45.69	534.04	47.21	713.19	48.94	903.55	51.48
372.76	46.01	545.09	47.26	724.82	49.32	924.16	51.93
383.52	46.13	556.16	47.55	747.81	49.32	936.58	52.15
394.30	46.43	567.07	47.65	759.65	49.62	949.04	52.03
405.06	46.39	577.83	47.55	771.73	49.91	960.00	52.35
415.81	46.31	588.62	47.87	783.23	50.14	970.00	52.53
426.52	46.43	599.56	47.88	795.14	50.24	980.00	52.71
437.23	46.74	610.54	47.97	807.10	50.61	990.00	52.90
447.94	46.88	621.52	47.93	819.07	50.39	999.99	53.09
458.67	46.96	632.67	48.08				

Table 3. Enthalpy of transition determinations of U_3As_4 and U_3Sb_4

Designation	T_1 K	T_2 K	$H(T_2) - H(T_1)$	
			$H(215\text{ K}) - H(179\text{ K})$ cal mole ⁻¹	$H(215\text{ K}) - H(179\text{ K})$ cal mole ⁻¹
U_3As_4				
Det'n A	179.28	214.57	1731.6	1765.0
Det'n B	179.57	214.86	1730.6	1765.8
Det'n D	179.98	215.27	1728.5	1765.3
			Mean: (1765.4 ± 0.4)	
U_3Sb_4				
			$H(175\text{ K}) - H(132\text{ K})$ cal mole ⁻¹	
Det'n A	132.15	172.17	1895.01	2025.6
Det'n B	132.52	172.69	1897.60	2023.8
Det'n D	132.10	173.92	1972.74	2024.8
			Mean: (2024.7 ± 1.1)	

with maxima at 196.1 K for U_3As_4 and 147.5 for U_3Sb_4 .

At the lowest temperatures the heat-capacity data were smoothed with the aid of plots of C_p/T vs T^2 and the functions evaluated by extrapolation of this line. In either compound the magnitudes of these extrapolations are only small fractions of the totals at 298.15 K. From these plots the values of the electronic heat-capacity coefficients, γ , were found to be 0.9×10^{-3} and 0.4×10^{-3} cal K⁻² mole⁻¹ for U_3As_4 and U_3Sb_4 , respectively.

The experimental heat capacities for both the low- and high-temperature regions were fitted to polynomials in temperature by least squares. Within the transition region the heat-capacity values were read from a large-scale plot and the thermodynamic functions were calculated by numerical integration of the curve by Simpson's rule or by direct enthalpy increment determinations. The curves were then integrated to yield values of thermodynamic functions at selected temperatures presented in Tables 4 and 5.

The thermodynamic functions are considered to have a precision indicated by a probable error less than 0.1% from 100 to 350 K and 0.3% at higher temperatures. An additional digit beyond those considered significant is given in Tables 4 and 5 for consistency and to permit interpolation and differentiation. The entropies and Gibbs energies have not been adjusted for nuclear spin and isotope mixing contributions and are thus practical values for use in chemical thermodynamic calculations.

In Table 6 are Curie temperatures, enthalpies and entropies of transition given for U_3As_4 , U_3Sb_4 and U_3P_4 .

DISCUSSION

It is well known that the magnetic contribution to the heat capacity cannot easily be resolved from the total heat capacity [24]. As heat-capacity data for diamagnetic Th_3As_4 and Th_3Sb_4 are not available, our estimate of ΔS

Table 4. Thermodynamic functions of U_3As_4 (cal = 4.184 J, molar mass/g = 1013.77)

T K	C_p cal K ⁻¹ mole ⁻¹	S° cal K ⁻¹ mole ⁻¹	$\{H^\circ(T) - H^\circ(0)\}$ cal mole ⁻¹	$-\{G^\circ(T) - H^\circ(0)\}/T$ cal K ⁻¹ mole ⁻¹
5	0.084	0.058	0.161	0.026
10	0.382	0.189	1.189	0.070
15	1.181	0.473	4.826	0.152
20	2.673	1.001	14.178	0.292
25	4.726	1.810	32.503	0.510
30	7.026	2.874	61.84	0.812
35	9.351	4.132	102.79	1.195
40	11.729	5.534	155.44	1.648
45	14.193	7.058	220.26	2.164
50	16.60	8.679	297.27	2.733
60	21.09	12.110	486.17	4.008
70	25.06	15.67	717.3	5.418
80	28.54	19.25	985.7	6.923
90	31.53	22.78	1286.5	8.489
100	34.08	26.24	1614.9	10.093
110	36.32	29.60	1967.1	11.714
120	38.41	32.85	2340.9	13.340
130	40.41	36.00	2750.0	14.963
140	42.31	39.07	3148.7	16.58
150	44.14	42.05	3581.0	18.17
160	45.98	44.96	4031.5	19.76
170	47.93	47.80	4500.9	21.32
180	50.14	50.60	4991.1	22.87
190	52.98	53.38	5505.5	24.40
196.08†	(57.64)	55.10	5837.6	25.32
200	46.64	56.06	6028	25.92
210	44.78	58.28	6482	27.41
220	44.38	60.35	6928	28.86
230	44.25	62.32	7371	30.27
240	44.27	64.21	7814	31.65
250	44.39	66.02	8257	32.99
260	44.50	67.66	8702	34.29
270	44.59	69.44	9147	35.56
280	44.67	71.06	9593	36.80
290	44.75	72.63	10040	38.01
300	44.84	74.15	10488	39.19
310	44.92	75.62	10937	40.34
320	45.00	77.05	11387	41.47
330	45.08	78.44	11837	42.57
340	45.16	79.78	12288	43.64
350	45.24	81.09	12740	44.64
400	45.63	87.16	15012	49.63
450	46.00	92.56	17303	54.10
500	46.36	97.42	19610	58.20
550	46.73	101.86	21940	61.97
600	47.10	105.94	24280	65.46
650	47.47	109.72	26650	68.72
700	47.81	113.25	29030	71.78
750	48.13	116.6	31430	74.66
800	48.46	119.7	33840	77.37
850	48.85	122.6	36280	79.95
900	49.36	125.4	38730	82.40
950	50.01	128.1	41220	84.74
1000	(50.61)	(130.7)	(43730)	(86.97)
273.15	44.61	69.96	9288	35.96
298.15	44.82	73.87	10405	38.97

†Peak of transition.

is, necessarily, somewhat arbitrary. Stalinski *et al.*[15] used the Heisenberg theory of spin-wave interactions[25] to estimate the magnetic heat capacity below $T_C/2$ for U_3P_4 , but as pointed out by de Jongh and Miedema[26] this method is only rigorous for insulating ferromagnets.

U_3Sb_4 is reported to be metallic and neutron diffraction measurements favor a non-collinear alignment of the spins[4, 12]. Henkie and Bazan[13] interpreted their

magnetoresistivity vs temperature data in terms of polyaxial structures for U_3P_4 and U_3As_4 .

The lattice heat capacities for U_3As_4 and U_3Sb_4 at constant volume were generated from θ_{Debye} values of 240 and 190 K, obtained as the maxima of the effective θ_{Debye} vs temperature curves below the transitions. A dilational contribution $C_d = C_p - C_v$ was estimated from the Nernst-Lindemann expression[27] $C_d = AC_p^2(T/T_m)$

Table 5. Thermodynamic functions of U_3Sb_4 (cal = 4.184 J, molar mass/g = 1201.09)

T K	C_p cal K ⁻¹ mole ⁻¹	S° cal K ⁻¹ mole ⁻¹	$\{H^\circ(T) - H^\circ(0)\}$ cal mole ⁻¹	$-\{G^\circ(T) - H^\circ(0)\}/T$ cal K ⁻¹ mole ⁻¹
5	0.086	0.046	0.142	0.018
10	0.534	0.201	1.375	0.063
15	1.969	1.654	7.198	0.174
20	4.290	1.521	22.551	0.393
25	7.161	2.779	51.01	0.739
30	10.317	4.361	94.64	1.207
35	13.515	6.192	154.24	1.786
40	16.67	8.204	229.73	2.461
45	19.71	10.344	320.74	3.217
50	22.54	12.569	426.45	4.040
60	27.43	17.13	677.1	5.840
70	31.45	21.67	972.1	7.778
80	34.88	26.10	1304.2	9.792
90	37.81	30.38	1668.1	11.843
100	40.35	34.49	2059.1	13.904
110	42.77	38.45	2474.7	15.96
120	45.26	42.28	2914.8	17.99
130	47.91	46.00	3380.3	20.00
140	51.19	49.67	3874.8	21.99
147.48†	(57.70)	52.45	4273.9	23.47
150	46.40	53.28	4396.6	23.97
160	44.11	56.17	4845	25.89
170	43.65	58.83	5505	26.45
180	43.62	61.32	5720	29.54
190	43.69	63.68	6156	31.28
200	43.76	65.92	6593	32.95
210	43.85	68.06	7032	34.57
220	43.95	70.10	7471	36.14
230	44.06	72.06	7911	37.66
240	44.18	73.93	8352	39.13
250	44.30	75.74	8794	40.56
260	44.43	77.48	9238	41.95
270	44.57	79.16	9683	43.30
280	44.72	80.78	10129	44.61
290	44.86	82.35	10577	45.88
300	45.01	83.88	11026	47.12
310	45.15	85.35	11477	48.33
320	45.30	86.79	11930	49.51
330	45.44	88.19	12383	50.61
340	45.58	89.55	12838	51.79
350	45.72	90.87	13295	52.88
400	46.31	97.01	15596	58.02
450	46.76	102.50	17924	62.67
500	47.12	107.44	20270	66.90
550	47.46	111.95	22630	70.79
600	47.86	116.09	25020	74.40
650	48.36	119.94	27420	77.76
700	48.96	123.6	29860	80.90
750	49.59	127.0	32320	83.86
800	50.22	130.2	34820	86.65
850	50.83	133.2	37340	89.30
900	51.46	136.2	39900	91.82
950	52.20	139.0	42490	94.23
273.15	44.62	79.68	9823	43.71
298.15	44.98	83.60	10943	46.89

†Peak of transition.

in which $A = 0.0212$ K mole cal⁻¹ and T_m is the melting temperature of the compounds taken as 1700 K [28]. The quantity $C_v + C_d$ was then subtracted from the observed heat capacities to give the total electronic heat capacities shown in Fig. 3. This arises from the cooperative (magnetic) contribution and the excitation of additional electronic levels. The excess entropies are shown as a function of temperature in Fig. 4. The excess entropy for U_3P_4 , which has been calculated from heat-capacity values given in Refs. [14] and [15], is plotted as well.

The same lattice estimation method was used for U_3P_4 with an effective θ_{Debye} of 300 K and a melting temperature taken as 1400 K [8]. In Fig. 4 the excess entropy curves for U_3As_4 and U_3Sb_4 are seen to approach the limiting value $\Delta S_i = R \ln(2J+1) = R \ln 9$ for the 3H_4 ground term of the U^{4+} ion at high temperatures. The very low excess entropy of U_3P_4 might be compensated by a larger contribution at higher temperatures but heat-capacity data for U_3P_4 above 350 K are, unfortunately, not available.

Table 6. Thermodynamic quantities for uranium pnictides

Quantity	U ₃ P ₄ [†]	U ₃ P ₄ [‡]	U ₃ As ₄	U ₃ Sb ₄
$C_p(298\text{ K})/\text{cal K}^{-1}\text{ mole}^{-1}$	41.85	42.74	44.82	44.98
$S^\circ(298\text{ K})/\text{cal K}^{-1}\text{ mole}^{-1}$	61.83	62.24	72.63	83.60
T_i/K	136.5	138.3	196.1	147.5
$\Delta H_f/\text{cal mole}^{-1}$	192	344	447.2	870
$\Delta S_f/\text{cal K}^{-1}\text{ mole}^{-1}$	1.50	3.09	6.7	6.8
$\Delta S_f^\circ/\text{cal K}^{-1}(\text{mole of U})^{-1}$	0.50	1.03	2.2	2.3
$\Delta S_f^\circ/\text{cal K}^{-1}(\text{mole of U})^{-1}$	0.61	0.59		

†Ref. [14].

‡Ref. [15].

§Recalculated with our lattice estimation.

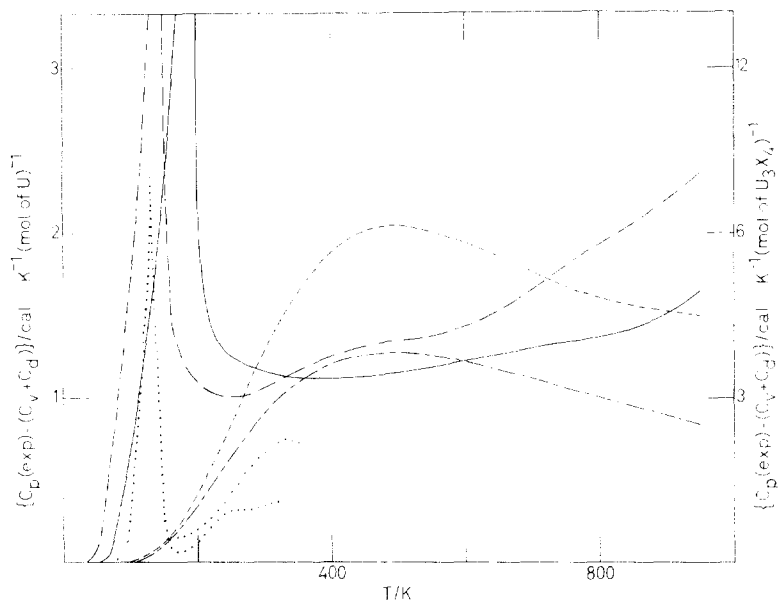


Fig. 3. Total magnetic heat capacities $C_p(\text{exp}) - (C_v + C_d)$ for U₃As₄ —, for U₃Sb₄ ---, and U₃P₄ (The lower curve is from Ref. [14] and upper from Ref. [15]). C_{Schottky} calculated for the electronic levels given by Troc *et al.* [3] ----, C_{Schottky} , fitted curve (see text) - - - - -.

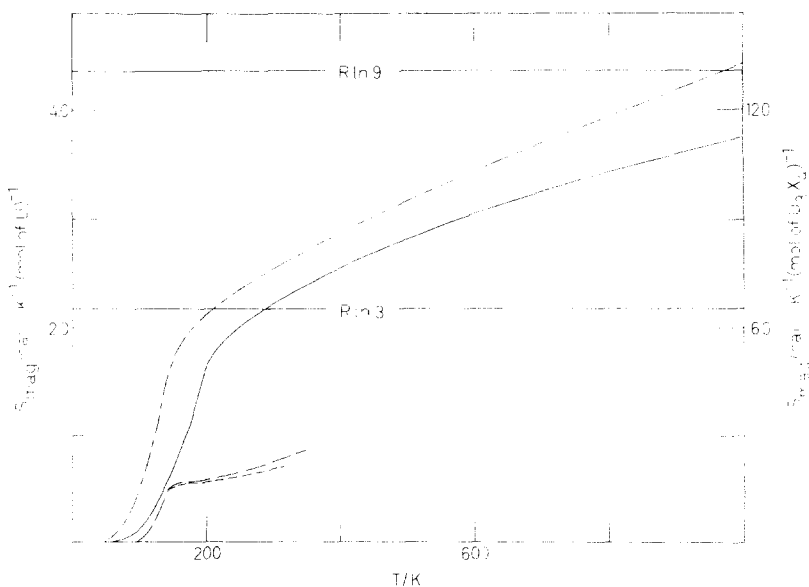


Fig. 4. Temperature dependence of the total magnetic entropy of $\frac{1}{3}\text{U}_3\text{As}_4$ —, for $\frac{1}{3}\text{U}_3\text{Sb}_4$ ----, for $\frac{1}{3}\text{U}_3\text{P}_4$ (Ref. [14]) ----, for $\frac{1}{3}\text{U}_3\text{P}_4$ (Ref. [15]) - - - - -.

Once the total magnetic heat capacity is established the problem remains of resolving the cooperative and non-cooperative contributions to the heat capacities. At temperatures above $3/2 T_C$ the contribution from residual ordering is probably of little importance compared with the Schottky heat capacity. It is therefore reasonable to assume that the excess entropy below this temperature is a fair approximation of the cooperative entropy. The entropies of transition of the three compounds are then found to be:

U_3P_4 (Ref. [14]):

$$S_{\text{exp}}(210 \text{ K}) - S_{\text{lattice}}(210 \text{ K}) = \Delta S_i \approx 0.61 \dagger \text{ cal K}^{-1} \text{ mole}^{-1}$$

U_3P_4 (Ref. [15]):

$$S_{\text{exp}}(210 \text{ K}) - S_{\text{lattice}}(210 \text{ K}) = \Delta S_i \approx 0.59 \dagger \text{ cal K}^{-1} \text{ mole}^{-1}$$

U_3As_4 :

$$S_{\text{exp}}(300 \text{ K}) - S_{\text{lattice}}(300 \text{ K}) = \Delta S_i \approx 2.2 \text{ cal K}^{-1} \text{ mole}^{-1}$$

U_3Sb_4 :

$$S_{\text{exp}}(225 \text{ K}) - S_{\text{lattice}}(225 \text{ K}) = \Delta S_i \approx 2.3 \text{ cal K}^{-1} \text{ mole}^{-1}$$

†Using our estimate of the lattice heat capacity.

The very large discrepancy between the ΔS_i values given in Refs. [14 and 15], 0.51 and 1.03 cal K⁻¹ mole⁻¹ respectively, is obviously due to the difference in lattice estimates by those authors.

These values are much smaller than would be expected from the 9-fold degeneracy of the 3H_4 ground term for the U^{4+} ion, but as pointed out by Counsell *et al.* [29] such low ΔS_i values can be evidence of crystal-field effects.

For U_3As_4 and U_3Sb_4 the values are close to $R \ln 3 = 2.2 \text{ cal K}^{-1} \text{ mole}^{-1}$, indicating that at the transition temperature essentially only three magnetic states per uranium atom are populated.

Troc *et al.* [3] calculated the crystal-field splitting for U_3P_4 and obtained reasonable agreement with their high-temperature magnetic-susceptibility data. The corresponding Schottky heat capacity was calculated for the electronic levels given † and is depicted in Fig. 3. Troc *et al.* assumed that at the transition temperature essentially only two low-lying singlets were populated. The ΔS_i values indicate however that three levels are populated at the transition temperature. Therefore, we fitted the excess heat-capacity curve with a triplet as the lowest level. The best fit is shown in Fig. 3 and is obtained using the following levels and degeneracies $|E_i(\text{hc})^{-1}/\text{cm}^{-1}, g_i|$: [0, 3], [750, 4], [1600, 2].

A model that does not require assumptions about a definite ionic state and allows for the essential interdependence of magnetic and conduction phenomena has been proposed by Robinson and Erdős [31]. The model takes into account the closeness of the 5f and 6s levels of uranium. This model has been successful in explaining the electronic and magnetic transition in UP, but this model cannot be applied in a straightforward manner to U_3As_4 and U_3Sb_4 since the resistivity vs temperature curves are very different from those for uranium mononictides.

†These levels and degeneracies $|E_i(\text{hc})^{-1}/\text{cm}^{-1}, g_i|$ are: [-803.5, 1], [-794.6, 1], [-93.3, 2], [+119.7, 1], [+318.5, 1], [426.9, 2], [492.8, 1].

Acknowledgements—The authors acknowledge with gratitude the partial financial support of the Chemical Thermodynamics Program in the Chemistry Section of the National Science Foundation as well as the assistance at Oslo of Tore Olsen in the preparation of samples and of Bjørn Lyng Nielsen in the calorimetric measurements. A travel grant from Kungliga Fysiografiska Sällskapet for Bengt Falk and to the Brazilian Research Council (CNPq) and to Universidade Federal de Santa Catarina for Affonso Alles are gratefully acknowledged.

REFERENCES

1. A. J. Freeman and T. B. Darby, Jr., *The Actinides: Electronic Structure and Related Properties*, Vols. I and II. Academic Press, New York (1974).
2. W. Trzebiatowski, A. Sepichowska and A. Zygmunt, *Bull. Acad. Polon. Sci., Ser. Sci. Chim.* **12**, 687 (1964).
3. R. Troc, J. Mulak and W. Suski, *Phys. Status Solidi (b)* **43**, 147 (1971).
4. Z. Smetana, V. Sechovsky and A. Menovsky, *Phys. Status Solidi (a)* **27**, K73-75 (1975).
5. R. Troc, W. Suski and C. Bazan, In *Conf. Dig. No. 3, Rare Earths and Actinides, Durham*, Inst. Phys. London and Bristol, pp. 172-175 (1971).
6. C. F. Buhner, *J. Phys. Chem. Solids* **30**, 1273 (1969).
7. C. E. Olsen and W. C. Koehler, *J. Appl. Phys.* **40**, 1135 (1969).
8. W. Trzebiatowski and R. Troc, *Bull. Acad. Polon. Sci., Ser. Sci. Chim.* **11**, 661 (1963).
9. S. Nasu, *Phys. Status Solidi (a)* **9**, 629 (1972).
10. J. Sternberk, J. Hrebik, A. Menovsky and Z. Smetana, *J. Phys. (Paris) Suppl.* **32**, 744 (1971).
11. W. Trzebiatowski and A. Zygmunt, *Bull. Acad. Polon. Sci., Ser. Sci. Chim.* **14**, 495 (1966).
12. R. Ciszewski, A. Murasik and R. Troc, *Phys. Status Solidi* **10**, K85 (1965).
13. Z. Henkie and C. Bazan, *Phys. Status Solidi (a)* **5**, 259 (1971).
14. J. F. Counsell, R. M. Dell, A. R. Junkison and J. F. Martin, *Trans. Far. Soc.* **63**, 72-79 (1967).
15. B. Stalinski, Z. Bieganski and R. Troc, *Phys. Status Solidi* **17**, 837 (1966).
16. M. R. Zaki and F. Grønvd, Personal communication (Jan. 1977).
17. F. Grønvd, M. R. Zaki, E. F. Westrum, Jr., J. A. Sommers and D. B. Downie, *J. Inorg. Nucl. Chem.* [Submitted].
18. P. G. Hambling, *Acta Cryst.* **6**, 98 (1953).
19. A. Iandelli, *Atti Acad. Naz. Lincei, Rend. Classe Sci., Mat. e Nat.* **13**, 144 (1952).
20. I. H. Warren and C. E. Price, *Can. Met. Quart.* **3**, 245 (1964).
21. R. Ferro, *Atti Acad. Naz. Lincei, Rend. Classe Sci., Mat. e Nat.* **13**, 53 (1952).
22. E. F. Westrum, Jr., G. T. Furukawa and J. P. McCullough, In *Experimental Thermodynamics*, (Edited by J. P. McCullough and D. W. Scott), Vol. I. Butterworths, London (1968).
23. Grønvd, F. *Acta Chem. Scand.* **21**, 1695 (1967).
24. E. F. Westrum, Jr. and W. G. Lyon, *Proc. Conf. Vienna. IAEA, Vienna* (1968).
25. F. J. Dyson, *Phys. Rev.* **102**, 1230 (1956).
26. L. J. de Jongh and A. R. Miedema, *Adv. in Physics* **23**, 14 (1974).
27. W. Nernst and F. A. Lindemann, *Z. Elektrochemie* **18**, 265 (1911).
28. B. J. Beadry and A. H. Doane, *Trans. Met. Soc. AIME* **215**, 199 (1959).
29. J. F. Counsell, R. M. Dell and J. F. Martin, *Trans. Faraday Soc.* **62**, 1736 (1966).
30. J. M. Robinson and P. Erdős, *Phys. Rev. B.* **8**, 4333 (1973).